

Investigating the Photoelectrochemical Performance of WO₃-TiO₂ Nanorod Photoanodes in Water Splitting

Armin Hariri¹, Neda Gilani^{2*}, Javad Vahabzadeh Pasikhani¹

1. Fouman Faculty of Engineering, College of Engineering, University of Tehran, P.O. Box 43515-1155, 43516-66456, Iran.

2. Department of Chemical Engineering, Faculty of Engineering, University of Guilan, P.O. Box 41996-13776, Iran.

* Corresponding Author's E-mails: n.gilani@guilan.ac.ir

Abstract

TiO₂ nanorod as a superior nanostructure has attracted a lot of attention to exert in the photocatalytic and photoelectrocatalytic applications in recent years. Nevertheless, its practical usage is restricted by a number of limitations such as the large band gap energy, the low rate of photo-induced carriers generation and the high rate of charge carriers recombination. Therefore in this study, incorporation of TiO₂ nanorod with WO₃ is proposed as a suitable approach to overcome these defects. In this regard, WO₃-TiO₂ nanorod was constructed by a facile one pot hydrothermal method in two incessant steps and was then employed as a potent photoanode for photoelectrocatalytic hydrogen generation. The morphology, elemental compositions and optical properties were characterized by the FESEM, EDS and DRS analysis, respectively. Furthermore, voltammetry analyses were performed to assay the photoelectrochemical features of WO₃-TiO₂ nanorod. The results confirmed that the incorporation of TiO₂ nanorod with WO₃ not only significantly made the band gap energy narrower (from 3eV to 2eV), but also dramatically intensified the photocurrent density and photoconversion efficiency from 1mA.cm⁻² to 1.8mA.cm⁻² and from 0.3% to 0.45%, respectively. As a consequence of improving optical properties and photoelectrochemical features, WO₃-TiO₂ nanorod could generate 2.43 mmol H₂ during 100 min under UV irradiation, which was 1.71 times more than hydrogen generated over pure TiO₂ nanorod.

Keywords: TiO₂ nanorods; Tungsten trioxide; Photoelectrochemical; Water splitting.

Introduction

Nowadays, the demand for adequate energy has increased as a consequence of rapid population growth along with economic developments in modern societies. Currently, most of the world's energy needs are supplied through fossil resources [1]. In this regard, the primary concern of consuming fossil fuels is the emission of harmful greenhouse gases, like carbon dioxide and nitrous oxide. To overcome this issue, the utilization of renewable hydrogen sources has been proposed as an alternative approach in recent years [2]. Among the various methods to generate hydrogen molecules, photoelectrocatalytic water splitting is considered as the most promising procedure due to the fact that it is cost-effective and eco-friendly [3]. In a conventional photoelectrocatalytic process, the water is oxidized at the photoanode to generate oxygen while hydrogen is generated at the cathode by reduction of water or generated protons from photoanode. Therefore, engaging a suitable photocatalyst to use as the photoanode is a key

factor in photoelectrocatalytic water splitting. It is worth noting that the water reduction reaction occurs at 0 V vs. NHE (H^+/H_2) while the water oxidation reaction happens at 1.23 V vs. NHE (H_2O/O_2) [4]. Consequently, the conduction band of the photocatalyst needs to be at a potential less than 0 V while the valence band needs to be at a potential more than 1.23 V.

Up to now, a wide range of semiconductors such as TiO_2 , ZnO, Fe_2O_3 , $BiVO_4$, WO_3 , CdS, and GaN have been used for the hydrogen production in photoelectrocatalytic systems. Among the different semiconductors, TiO_2 nanorod is renowned as a good candidate for photoelectrocatalytic hydrogen production due to its unique characteristics such as appropriate energy band position, super hydrophilicity, non-toxicity, high chemical stability and low cost [5]. However, the wide band gap energy of TiO_2 nanorods, which is in the range of 3eV to 3.2eV, has restricted its photocatalytic activity under visible light irradiation. In addition, the rapid charge recombination is another drawback that has limited the practical photoelectrocatalytic hydrogen generation [2,3,5]. To offset these drawbacks, doping TiO_2 nanorods with metals, non-metals or coupling with a second semiconductor with the lower band gap energy are suggested as a proper solution. Accordingly, Tungsten is a predominant dopant since it has a high charge state with six electrons in the outer orbit and ionic radius with a value of 0.60 Å. Since the ionic radius of Tungsten is similar to the ionic radius of Titanium (0.605 Å), W atoms can facilitate substitute with the Ti^{4+} atoms in TiO_2 lattices. Furthermore, incorporation of WO_3 and TiO_2 not only reduces the band gap of TiO_2 nanorods, but also significantly inhibits the recombination of photo-generated charge carriers [3].

Therefore, the primary purpose is fabricating incorporated TiO_2 nanorods with WO_3 nano particles and investigating their ability for Photoelectrochemical hydrogen generation. For this purpose, WO_3 - TiO_2 nano rod were constructed by one pot hydrothermal method. Meanwhile the photoelectrochemical properties as well as physicochemical features were investigated by voltammetry analyses, FESEM, EDS and DRS, respectively.

Experimental

1-Preparation of WO_3 -TNRs

To start, Ti sheets (99%) were chemically polished in a mixture of HF, HNO_3 and distilled water solutions with a volume ratio of 1:4:5. The polished Ti sheets were pretreated by soaking in the $TiCl_4$ aqueous solution at 70 °C for 50 min. After washing pretreated Ti sheets with deionized water, they were annealed at 450 °C for 1h. In the next step, the hydrothermal method was employed to create TiO_2 nanorods (TNRs) as follows: 30 ml H_2O and 30 ml HCl (36.5-38 wt.%) were mixed with 6 ml methanol. Subsequently, 0.23 g PA was added in the above solution under stirring for 10 min. Then 0.5 ml TBT was added under vigorous stirring. Afterward, the mixture and pretreated Ti sheet were transferred to a Teflon vessel to carry out the hydrothermal reaction at 160°C for 12 h. Eventually, after cooling down the Teflon vessel to room temperature, the as-fabricated TNRs were rinsed with distilled water and calcined in air at 450°C for 2 h with a heating rate of 3°C/min.

To synthesis WO_3 -TNRs, 0.01 mg WCl_6 was dissolved in 70 ml methanol under stirring. Subsequently, the TNRs sheet were placed in the solution and was then exposed to ultrasonic treatment for 30 min. The solution and TNRs sheet was then transferred into 100 ml Teflon vessel and heated at 180 °C for 3h. Finally, after cooling down to room temperature, the WO_3 -TNRs was calcined at 450 °C for 1h under atmosphere condition.

2- Characterization

The morphology and structural properties of the as-synthesized samples were determined by a field-emission scanning electron microscopy (FESEM; Hitachi S4160, Japan) and the elemental composition was estimated by energy dispersive X-ray spectroscopy (EDX). The optical feature of TNRs and WO_3 -TNRs was investigated by Diffuse Reflectance UV–vis Spectrophotometer (DRS, Shimadzu, Japan).

3- Photoelectrochemical experiments

The photoelectrochemical performance was measured using potentiostat/galvanostat (PGS-8, Sharif Solar, Iran) in 0.1M Na₂SO₄ electrolyte with a standard three-electrode cell consisting of the achieved TiO₂ nanorods, platinum foil, and Ag/AgCl as the working, counter and reference electrodes, respectively. The working electrode (active area: 8 cm²) was illuminated by a UV light source (315–400 nm) with the light intensity of 100 mWcm⁻². All the photoelectrochemical measurements were performed for general presentation under air condition.

4- Hydrogen production performance

The evolution of hydrogen was performed through the water splitting in a two compartment photoelectrochemical cell (PEC). In this regard, the PEC cell was separated by a Nafion membrane into two detached chambers namely, an anodic chamber and a cathodic chamber, in which each chamber was filled with 0.1 M Na₂SO₄ electrolytes. The synthesized WO₃-TNRs, Ag/AgCl and Ti sheet served as photoanode, reference electrode and cathode, respectively. The hydrogen was generated on the cathodic chamber by applying 1 V bias voltage vs. Ag/AgCl under UV irradiation. An inverted burette with displacing electrolyte in the burette column was employed to collect the generated hydrogen gas at the cathode. The volume of H₂ was directly determined by reading the changes in the electrolyte level.

Results and discussion

1-FESEM & EDS & DRS

To investigate the morphology and structure of as-prepared TNRs and WO₃-TNRs the FESEM analysis was performed. The FESEM images of TNRs and WO₃-TNRs are presented in Fig. 1(a) and 2(a), respectively. Fig. 1(a) and Fig. 2(a), indicate that the nanorods synthesized by the hydrothermal method have smooth and monotonic outer surfaces with quadrilateral vertices. In comparison with Fig. 1(a), no alteration was witnessed in the morphology and structural properties of WO₃-TNRs (Fig. 2(a)). Consequently, the hydrothermal procedure is a proper way for the incorporation of WO₃ and TiO₂ nanorods.

To identify the elements that exist in both TNRs and WO₃-TNRs photocatalysts, the EDS analysis was performed and the results are exhibited in Fig. 1(b) and 2(b), respectively. Based on these figures, Ti and O atoms are the dominant elements in both photocatalysts. Furthermore, based on Fig. 2(b), the distinguished peaks of WO₃-TNRs around 1.8, 7.2, 8.2 and 9.4 keV prove the prosperous embedment of W atoms instead of Ti atoms. Fig. 1(c) and 2(c) shows the UV–vis diffuse reflectance absorption spectra (DRS) of TNRs and WO₃-TiO₂ nanorods. DRS studies help to understand the band gaps of the material. The value of band gap of the samples can be estimated through equation [5]:

$$(\alpha h\nu)^{0.5} = A(h\nu - E_g)$$

where E_g is the band gap energy of the material, h is Planck's constant, ν is the frequency of vibration, $h\nu$ is the energy of the incident photon, A is a proportional constant and α is the coefficient of absorption per unit length (cm⁻¹). Fig. 1(c) and 2(c) shows the plots of $(\alpha h\nu)^{0.5}$ vs. photon energy ($h\nu$). By considering equation, through extrapolating the linear portion of $(\alpha h\nu)^{0.5}$ versus photon energy ($h\nu$) plot to $\alpha \rightarrow 0$, E_g of the samples was obtained. Fig. 1(c) and 2(c) show the band gap value of TNRs and WO₃-TNRs. The band gap energies decreased dramatically from 3 eV for TNRs to 2 eV for WO₃-TNRs. By coupling TNRs with W, we were able to lower the band gap energy of TNRs to a lower value and improve efficiency in the visible area.

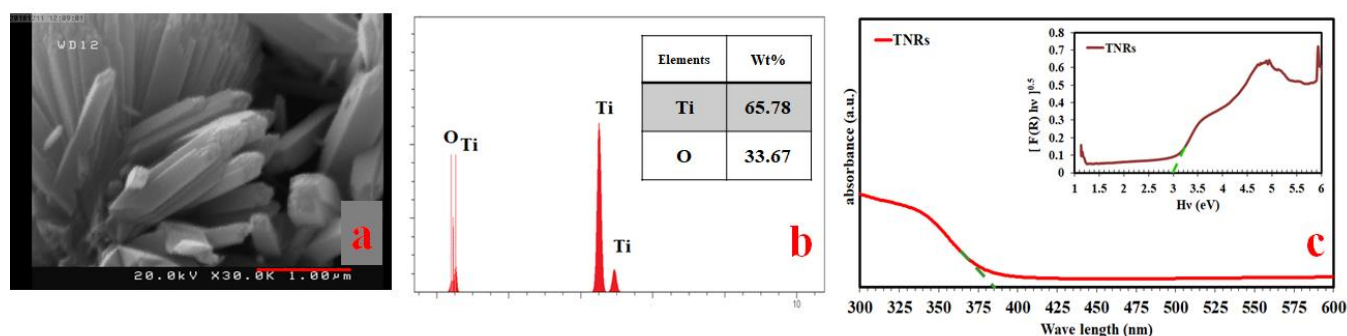


Fig.1. a) FESEM of TNRs, b) EDS of TNRs, c) DRS analysis

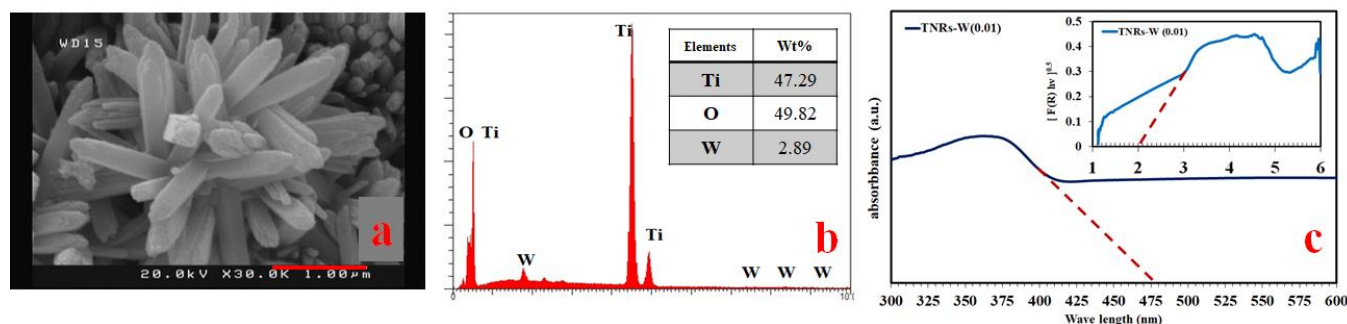


Fig. 2. a) FESEM of TNRs-W, b) EDS of TNRs-W, c) DRS analysis

2- Photoelectrochemical measurement

Photocurrent measurement was used to evaluate the charge separation in the as-prepared photocatalysts. In this regard, larger photocurrent means higher separation efficiency and more photo-generated electrons. The characteristics of photocurrent density-voltage (j - V) curves were recorded under UV light and the results are displayed in Fig 3(a). As shown in Fig 3(a), tungsten has a significant effect on photocurrent density. The photocurrent density of WO_3 -TNRs was 1.875 mA/cm^2 at 1V vs. Ag/AgCl that it was 1.87 times more than the photocurrent density of TNRs. This result confirms that the photo-generated electrons on the WO_3 -TNRs can be faster transported to the counter electrode, and great water splitting efficiency can be expected. Fig 3(b) shows the transient photocurrent density of TNRs and WO_3 -TNRs photoelectrodes by several on-off cycles under UV light. It can be seen that the photocurrent went down to zero as soon as the irradiation of light was stopped, while subsequently shifted to original value as soon as the light switched on again. This result implies the superior responsibility of both photoanodes to the photon energy, the effective charge transfer and electron collection within the photoelectrochemical cell. Moreover, the higher photocurrent density of WO_3 -TNRs as compared to TNRs photoanode, indicate that incorporation of TiO_2 nanorods with WO_3 is an excellent manner to decrease the electrons-holes recombination rate and enhance the charge transfer.

The hydrogen production efficiency (photoconversion efficiency) of the prepared samples is determined by the following equation [5]:

$$\eta (\%) = j_p \left[\frac{E_{rev}^0 - |E_{app}|}{I_0} \right] * 100$$

where η is the photoconversion efficiency, j_p is the photocurrent density (mA.cm^{-2}), I_0 means the intensity of the incident light, E_{rev}^0 represents the standard changeable potential (1.23 V vs. RHE), and $|E_{app}|$ denotes the absolute value of the applied voltage which is obtained from $E_{app} = E_{meas} - E_{aoc}$, where E_{meas} is the electrode potential (vs. Ag/AgCl) at which j_p is measured and E_{aoc} is the electrode potential (vs. Ag/AgCl) at open circuit under illumination. Plots of photoconversion efficiency with applied potential are presented in Fig. 3(c). Based on Fig 3(c), it can be observed that the incorporation of TNRs with WO_3 leads to a dramatic increase in the

photoconversion efficiency. In this regard, the maximum photoconversion efficiency of WO₃-TNRs is approximately 1.5 times more than pure TiO₂ nanorods.

To sum up, the photoelectrochemical results revealed that the incorporation of TNRs with WO₃ can intensify the photocurrent density and photoconversion efficiency under UV irradiation as well as prevent the recombination of electron-hole pairs. Therefore, more electrons can be transferred from photoanode to cathode and greater water splitting can be expected.

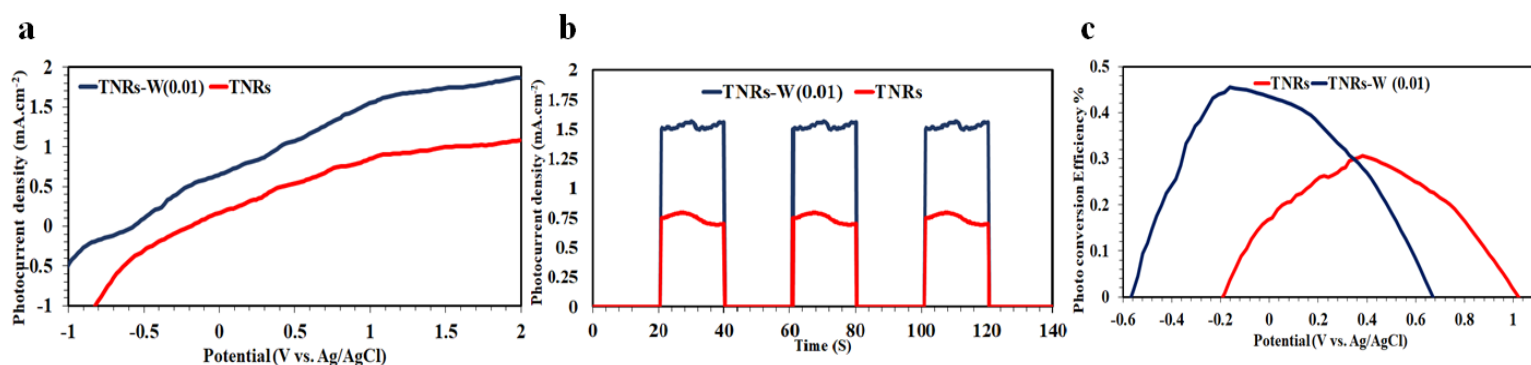


Fig 3. a) Photocurrent density of TNRs and TNRs-W under UV light, b) The transient photocurrent response curves of TNRs and TNRs-W at 1V vs. Ag/AgCl under UV light, c) Photo conversion efficiency of TNRs and TNRs-W

3-Photoelectrocatalytic performance

Fig.4(a) presents the amount of generated hydrogen by TNRs and TNRs-W. According to the results, the amount of generated hydrogen by TNRs-W was 2.4 mmol which was 1.7 times more than the amount of generated hydrogen by TNRs. Furthermore, the rate of hydrogen production (mmol·min⁻¹) was calculated with respect to the slopes obtained from the hydrogen mole-time curves Fig.4(a). As shown in Fig.4(b), it can be observed that the incorporation of TNRs with WO₃ increased the hydrogen production rate from 14.9 mmol·min⁻¹ to 24.3 mmol·min⁻¹.

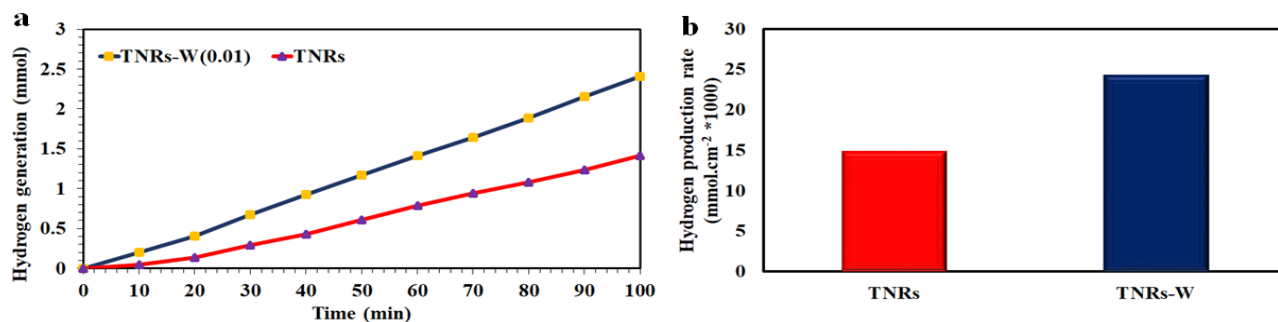


Fig.4. a) Hydrogen generation of TNRs and TNRs-W, b) hydrogen generation rate of TNRs and TNRs-W

To sum up, the results of photoelectrocatalytic hydrogen generation are in agreement with the results achieved from photoelectrochemical measurements. Incorporation of TiO₂ nanorod with WO₃ by promoting optical properties leads to further absorption of light, increasing photocurrent density, retarding the electron-hole pairs recombination and enhancing photoconversion efficiency. Therefore, the WO₃-TNRs photoanode can improve the photoelectrocatalytic hydrogen generation in comparison with the pure TiO₂ nanorode.

Conclusions

In summary, WO₃-TNRs were fabricated by the one pot hydrothermal method and were then employed as the suitable photoanodes for photoelectrochemical hydrogen generation. The FESEM and EDS results justified that hydrothermal procedure is a proper manner to efficiently incorporate WO₃ with TiO₂ nanorods without any alteration on its nanostructure. Furthermore, it was found that embedding Tungsten elements into TiO₂ nanorods lattices can reduce the band gap energy (from 3eV to 2eV) as well as increase the photocurrent density and

photoconversion efficiency from 1 mA.cm⁻² to 1.8mA.cm⁻² and from 0.3% to 0.45%, respectively. Meanwhile, the hydrogen generation rate was boosted significantly from 14.9 mmol.min⁻¹ to 24.3 mmol.min⁻¹, as a consequence of the improvement in both optical properties and photoelectrochemical features. Therefore, it can be concluded that the WO₃-TNRs photoanode would be a suitable alternative to utilize in PEC applications.

References:

- [1] Dincer, I. and Acar, C., "A review on clean energy solutions for better sustainability", Int. J. Energy Res., 39, 585-606 (2015).
- [2] Gilani, N., Pasikhani, J.V., Motie, P.T. and Akbari, M., "Fabrication of quantum Cu(II) nanodot decorated TiO₂ nanotubes by the photochemical deposition-assisted hydrothermal method: study catalytic activity in hydrogen generation", Desalin. Water Treat., 139, 145-155 (2019).
- [3] Momeni, M.M., Ghayeb, Y. and Davarzadeh, M., "Single-step electrochemical anodization for synthesis of hierarchical WO₃-TiO₂ nanotube arrays on titanium foil as a good photoanode for water splitting with visible light", J. Electroanal. Chem., 739, 149-155 (2015).
- [4] Hussain, E., Majeed, I., Amtiaz Nadeem, M., Badshah, A., Chen, Y., Arif Nadeem, M. and Jin, R., "Titania-Supported Palladium/Strontium Nanoparticles (Pd/Sr-NPs@P25) for Photocatalytic H₂ Production from Water Splitting. " J. Phys. Chem., 120, 17205-17213 (2016).
- [5] S. Shen, J. Chen, M. Wang, X. Sheng, X. Chen, X. Feng and S. S. Mao, "Titanium dioxide nanostructures for photoelectrochemical applications," Prog. Mater. Sci., 98, 299-385 (2018)
- [6] Pasikhani, J.V., Gilani, N. and Pirbazari, A. E., "Improvement the wastewater purification by TiO₂ nanotube arrays: The effect of etching-step on the photo-generated charge carriers and photocatalytic activity of anodic TiO₂ nanotubes", Solid State Sci., 84, 57-74 (2018).